About 2D Cavity Resonance

May 12, 2026
May 16, 2026 Revised
Takuya Yabu(takuya.yabu@live.jp)

Abstract

Research on automobile whistling and suction sounds has been conducted in the past. For cavity resonance, a type of whistling sound, the cavity resonance frequency has been determined using Rossiter's empirical equation. Therefore, we limited our study to the two-dimensional case and clarified the physical phenomena that arise by solving a set of partial differential equations that explain the phenomenon. As a result, we found that the horizontal resonance frequency becomes proportional to the speed of sound as the mainstream velocity increases, and the vertical resonance frequency decreases as the mainstream velocity increases, but when the Mach number exceeds 1, the resonance frequency no longer exists as a real number, and vertical resonance does not occur. Finally, we discussed the conditions under which resonance increases. Finally, we were able to confirm the conditions under which resonance increases through numerical calculations.

Nomenclature

L_H: Maximum hole length
ρ, c: Air density and air sound speed
ω: Angular frequency
f_x, f_y: x-direction resonance frequency and y-direction resonance frequency
k: Wavenumber
t: Time
j: Imaginary unit
U, U_{vx}: Mainstream air velocity and vortex (vorticity) velocity
κ: Ratio of vortex (vorticity) velocity to mainstream air velocity
ϕ: Empirical coefficient for phase lag
M: Mach number
ζ: Vorticity
β: Efficiency of conversion from sound pressure to vorticity
$\delta(x)$: Dirac delta function
$\delta'(x)$: Differential of Dirac delta function
$H(x)$: Heaviside step function

s: Complex number

L_y: Depth of the box

$u(x,y,t), v(x,y,t)$: Velocity in the x direction and velocity in the y direction

1. Introduction

In the past, research has been conducted on the whistling and suction sounds of automobiles (Calvo, Diaz, & San Roman, 2005) (Chien-Hsiung, Lung-Ming , Chang-Hsien , Yen-Loung , & Jik-Chang , 2009) (George, 1990) (Jagtiani, 1972) (Jung & Oh, 1995) (Münder & Carbon, 2022) (Oettle & Sims-Williams, 2017) (Qatu, Abdelhamid, Pang, & Sheng, 2009) (Wang, Chen, & Zhang, 2021) (Zhang, Meng, Li, & Zheng, 2022). Cavity resonance is a type of whistling sound. In cavity resonance, the cavity resonance frequency has traditionally been determined using Rossiter formula, an empirical formula. Therefore, for cavity resonance in the two-dimensional case, we will clarify the physical phenomena that arise by solving the set of partial differential equations that explain the phenomenon. Finally, we will examine the conditions under which resonance increases in numerical calculations.

These will be discussed below.

2. About 2D Cavity Resonance

2.1. Vorticity Movement Equation

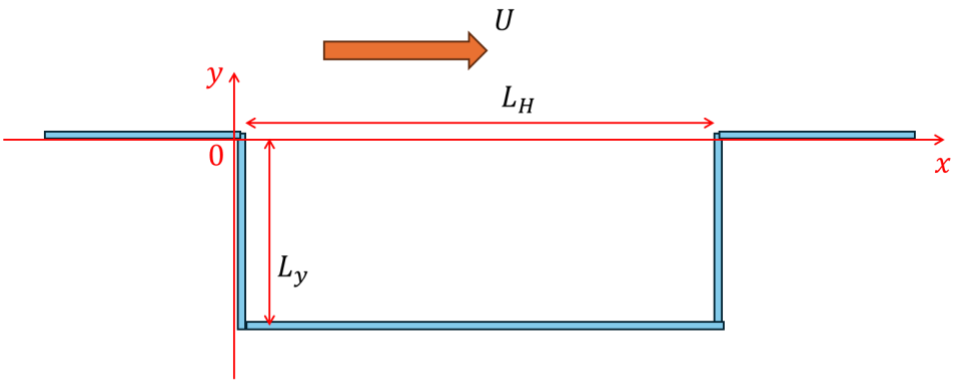

Fig. 1 2-Dimensional Box with Hole

Fig. 1 shows a box with a hole. Here, the conventional definitions of cavity resonance and cavity resonance frequency are given below.

Definition：

When air is flowing at velocity U and there is a hole, a vortex moves from

the upstream end to the downstream end of the hole. This vortex collides with the downstream end, generating sound. This generated sound then moves from the downstream end to the upstream end. Sound is a change accompanied by particle velocity, and this particle velocity then collides with the upstream end, generating another vortex. This series of phenomena is defined as "cavity resonance." Furthermore, the reciprocal of the time from when a vortex moves and generates sound until another vortex is generated is defined as the "cavity resonance frequency."

Based on this definition, we derive the differential equation representing cavity resonance, limited to two dimension. First, the movement equation of vorticity $\zeta(x, y, t)$ is expressed by the following equation. However, the viscosity term is ignored.

$$\frac{\partial \zeta}{\partial t} + U_{vx}\frac{\partial \zeta}{\partial x} = 0 \tag{1}$$

2.2. Powell's Equation

Next, we will find the relationship between sound pressure and vorticity.

Powell's equation is the relationship between sound pressure and vorticity. Expressed in two dimension, Powell's equation is given by the following:

$$\frac{1}{c^2}\frac{\partial^2 p}{\partial t^2} - \left(\frac{\partial^2 p}{\partial x^2} + \frac{\partial^2 p}{\partial y^2}\right)$$
$$= \rho[-\zeta(L_H, 0, t)v(L_H, 0, t)\delta'(x - L_H)\delta(y) + \zeta(L_H, 0, t)u(L_H, 0, t)\delta(x - L_H)\delta'(y)] \tag{2}$$

2.3. Initial Conditions

The initial condition for the velocity in the x-direction is given below:

$$u(x, y \geq 0, 0) = U \tag{3}$$

The initial condition for the velocity in the y-direction is given below:

$$v(x, y, 0) = 0 \tag{4}$$

The initial condition for the sound pressure is given below:

$$p(x, y, 0) = 0 \tag{5}$$

The initial condition for the time derivative of the sound pressure is given below:

$$\left.\frac{\partial p}{\partial t}\right|_{t=0} = 0 \tag{6}$$

2.4. Boundary Conditions

We need to find the boundary conditions under which the velocity of the returned particles changes to vorticity. These are given by the following equation:

$$\zeta(0,0.t) = -\beta_x \frac{\partial p}{\partial x}\Big|_{(x=0,y=0,t=t)} \tag{7}$$

Furthermore, assuming that the sound pressure is perfectly reflected at the bottom of the box, the following condition holds:

$$\frac{\partial p}{\partial x}\Big|_{y=-L_y} = 0 \tag{8}$$

Furthermore, assuming that the sound pressure is completely reflected by the left and right walls, the following conditions hold true.

$$\frac{\partial p}{\partial x}\Big|_{x=0,-L_y\le y\le 0} = 0 \tag{9}$$

$$\frac{\partial p}{\partial x}\Big|_{x=L_H,-L_y\le y\le 0} = 0 \tag{10}$$

3. Resonance Frequency of a Two-Dimensional Cavity Resonance

3.1. Solution to the Vorticity Transfer Equation

We derive the resonance frequency of a two-dimensional cavity resonance. First, we solve equation (1). The solution when the boundary condition is $\zeta(0,t)$ is given by the following equation:

$$\zeta(x,y,t) = \zeta\left(0,0,t-\frac{x}{U_{vx}}\right) \tag{11}$$

3.2. Sound Pressure Equation Using Green's Function Derived from Powell's Equation

Next, we solve Powell's equation (2). This can be obtained using the Green's function in the following form. First, the Green's function is given by the following equation.

$$G(x,y,t|L_H,0,\tau) = \sum_{n=-\infty}^{\infty}\left\{\frac{H\big(c(t-\tau)-r_{n,1}\big)}{2\pi c\sqrt{c^2(t-\tau)^2-r_{n,1}^2}} + \frac{H\big(c(t-\tau)-r_{n,2}\big)}{2\pi c\sqrt{c^2(t-\tau)^2-r_{n,2}^2}}\right\} \tag{12}$$

Here, the following equation holds true.

$$r_{n,1} = \sqrt{(x-(2n+1)L_H)^2+y^2} \tag{13}$$

$$r_{n,2} = \sqrt{(x-(2n+1)L_H)^2+\big(y+2L_y\big)^2} \tag{14}$$

From equations (2) and (12), the following equation is obtained.

$$p(x,y,t)=\sum_{n=-\infty}^{\infty}\int_{0}^{t-\frac{r_{n,1}}{c}}\frac{(-\rho\beta_x)\cdot\left.\frac{\partial p}{\partial x}\right|_{\left(0,0,\tau-\frac{L_H}{U_{vx}}\right)}\cdot\Phi_{n,1}(\tau)}{2\pi c\sqrt{c^2(t-\tau)^2-r_{n,1}^2}}d\tau$$

$$+\sum_{n=-\infty}^{\infty}\int_{0}^{t-\frac{r_{n,2}}{c}}\frac{(-\rho\beta_x)\cdot\left.\frac{\partial p}{\partial x}\right|_{\left(0,0,\tau-\frac{L_H}{U_{vx}}\right)}\cdot\Phi_{n,2}(\tau)}{2\pi c\sqrt{c^2(t-\tau)^2-r_{n,2}^2}}d\tau \tag{15}$$

Here, the following equation holds true.

$$\Phi_{n,1}(\tau)=\frac{v(L_H,0\,,\tau)\cdot(x-(2n+1)L_H)-(-1)^n\cdot U\cdot y}{c^2(t-\tau)^2-r_{n,1}^2} \tag{16}$$

$$\Phi_{n,2}(\tau)=\frac{v(L_H,0\,,\tau)\cdot(x-(2n+1)L_H)-(-1)^n\cdot U\cdot\left(y+2L_y\right)}{c^2(t-\tau)^2-r_{n,2}^2} \tag{17}$$

3.3. x-Direction Resonance Frequency

Consider the resonance frequency in the x-direction. The time it takes for vorticity to propagate downstream is $\frac{L_H}{U_{vx}}$, and the time it takes for the sound to return upstream is $\frac{L_H}{c}$. Here, the phase synchronization condition is assumed to be: "Let T_x be the period of the sound produced (frequency is $f_x=\frac{1}{T_x}$). The total time taken for one cycle, $\frac{L_H}{U_{vx}}+\frac{L_H}{c}$, is equal to an integer multiple (n_x times) of the sound period, taking into account the fluid-induced generation delay (phase difference ϕ)." In this case, the following equation holds:

$$\left(n_x-\frac{\phi}{2\pi}\right)T_x=\frac{L_H}{U_{vx}}+\frac{L_H}{c}$$

$$\frac{\left(n_x-\frac{\phi}{2\pi}\right)}{f_x}=\frac{L_H}{U_{vx}}+\frac{L_H}{c}$$

$$f_x=\frac{\left(n_x-\frac{\phi}{2\pi}\right)}{\frac{L_H}{U_{vx}}+\frac{L_H}{c}} \tag{18}$$

Finally, setting $U_{vx}=\kappa U$, we obtain the following equation. This is Rossiter formula.

$$f_x=\frac{U}{L_H}\frac{\left(n_x-\frac{\phi}{2\pi}\right)}{\left(\frac{1}{\kappa}+\frac{U}{c}\right)} \tag{19}$$

3.4. y-Direction Resonance Frequency

Consider the resonance frequency in the y-direction. The velocity vector of sound is carried along by the mainstream velocity U. If we let θ be the angle at which the sound wave propagates relative to the air, the actual sound wave vector $\overrightarrow{v_s}$ as seen from the ground is given by:

$$\begin{aligned}\overrightarrow{v_s} &= (U, 0) + (c\cos\theta, c\sin\theta) \\ &= (U + c\cos\theta, c\sin\theta)\end{aligned} \tag{20}$$

The condition for the sound wave vector to propagate perpendicularly is given by:

$$U + c\cos\theta = 0$$

$$\therefore \cos\theta = -\frac{U}{c} \tag{21}$$

The effective sound velocity c_y in the y-direction is given by:

$$\begin{aligned}c_y &= c\sin\theta \\ &= c\sqrt{1 - \cos^2\theta}\end{aligned}$$

$$\therefore c_y = c\sqrt{1 - \left(\frac{U}{c}\right)^2} \tag{22}$$

The basic formula for the y-direction resonance frequency f_y of a closed tube in stationary space is as follows:

$$f_y = \frac{n_y \cdot c}{2L_y} \tag{23}$$

By replacing c with the effective speed of sound c_y, the y-direction resonance frequency f_y can be found as follows:

$$f_y = \frac{n_y \cdot c_y}{2L_y}$$

$$\therefore f_y = \frac{n_y \cdot c}{2L_y}\sqrt{1 - \left(\frac{U}{c}\right)^2} \tag{24}$$

3.5. What Can Be Understood from the Resonance Frequency

By further transforming the x-direction resonance frequency in equation (19) as $U \to \infty$, the following equation is obtained:

$$f_x = \frac{U}{L_H}\frac{\left(n_x - \frac{\phi}{2\pi}\right)}{\left(\frac{1}{\kappa} + \frac{U}{c}\right)} \to \frac{\left(n_x - \frac{\phi}{2\pi}\right)}{L_H}c \tag{25}$$

That is, the x-direction resonance frequency becomes proportional to the speed of sound

as the mainstream velocity increases.

In equation (24), the y-direction resonance frequency includes the mainstream velocity as $\sqrt{1-\left(\frac{U}{c}\right)^2}$, so the frequency decreases as the mainstream velocity increases. Also, when $U > c$, that is, when the Mach number M is greater than 1, the square root becomes a complex number, so the y-direction resonance frequency does not exist as a real number, and no resonance occurs in the y-direction.

Furthermore, the sound pressure $p(x, y, t)$ is largest when $f_x = f_y$ At that time, the following condition is satisfied:

$$\frac{U}{L_H}\frac{\left(n_x - \frac{\phi}{2\pi}\right)}{\left(\frac{1}{\kappa}+\frac{U}{c}\right)} = \frac{n_y \cdot c}{2L_y}\sqrt{1-\left(\frac{U}{c}\right)^2} \tag{26}$$

From equation (26), the left side increases almost proportionally to U, and the right side decreases slightly with U. Only at a specific flow velocity U where these two curves intersect does the sound pressure p, which is the solution to this set of equations, have a large amplitude. Also, when the phase delay ϕ changes, the flow velocity at which resonance occurs shifts to the left or right. This indicates that the characteristics of the boundary condition β_x govern the timing of when the sound begins to resonate. Furthermore, the ratio of L_H to L_y determines whether the n_x-th-order mode or the n_y-th-order mode is preferentially selected.

4. Numerical Calculations

The results were confirmed by numerical calculation. The values used are shown in Table 1 below.

Furthermore, for $\frac{\partial p}{\partial x}$ and $v(L_H, 0, t)$, it was assumed that vortices were continuously generated at the upstream end at a Rossiter formula primary frequency of 14.4 Hz, and that this vortex mass was continuously excited at the downstream end as $v(L_H, 0, t)$ at the same Rossiter formula primary frequency of 14.4 Hz. Therefore, the following equation is continuously used during the numerical calculation. Here, $f_{x,1}$ is the Rossiter formula primary frequency of 14.4 Hz.

$$\frac{\partial p}{\partial x} = \sin\left(2\pi f_{x,1} t\right) \tag{27}$$

$$v(L_H, 0\,, t) = \frac{1}{2}\sin\left(2\pi f_{x,1} t\right) \tag{28}$$

Table 1 Parameter and Value

Parameter	Value
ρ	1.225(kg/m^3)
c	340.0(m/s)
U	34.0(m/s)
κ	0.6
β_x	0.01
ϕ	$\frac{\pi}{2}$
L_H	1.0(m)
L_y	0.5(m)

The numerical calculation results are shown in Fig. 2. The observation position was $(x, y) = (0.01, 0.01)$ near the origin. The top graph shows the time-series waveform of sound pressure, and the bottom graph shows the frequency characteristics of sound pressure.

Looking at the time-series waveform of sound pressure in Fig. 2, we can see that waveforms from various sound sources are combined and gradually increase in size as self-excited oscillations. In other words, it is clear that cavity resonance is self-excited.

Next, looking at the frequency characteristics of sound pressure in Fig. 2, we first see a peak at 14.4 (Hz), which is the first frequency of Rossiter formula f_x. There is also a peak at 338.3 (Hz), which is the first frequency of f_y indicating the resonance frequencies in the x and y directions. Furthermore, $\frac{f_y}{f_x}$=23.5, indicating that f_y is approximately 24 times the value of f_x. This means that, due to the strong nonlinear distortion caused by the square root denominator of the Green's function, when the energy at $n_x = 1$ (14.4 Hz) is distributed to harmonics, only the harmonics that are mathematically and phasely most compatible with the vertical eigenmode $n_y = 1$ created by $y = -L_y$—the harmonics that are multiples of 6 (6th, 12th, 18th, 24th)—are selectively drawn into the spatial resonant chamber and appear strongly.

In Fig. 2, a green dashed line is drawn at the positions of multiples of 6 of the frequency $f_x = 14.4$ (Hz), which is the frequency at $n_x = 1$. The property that the true time-domain integral (red peak) shifts neatly and consistently to the left (lower frequencies) relative to the green dashed line indicates a physical phenomenon where the "tail effect" (accumulation of past reverberations) unique to two-dimensional space

naturally increases the equivalent phase delay within the time integral.

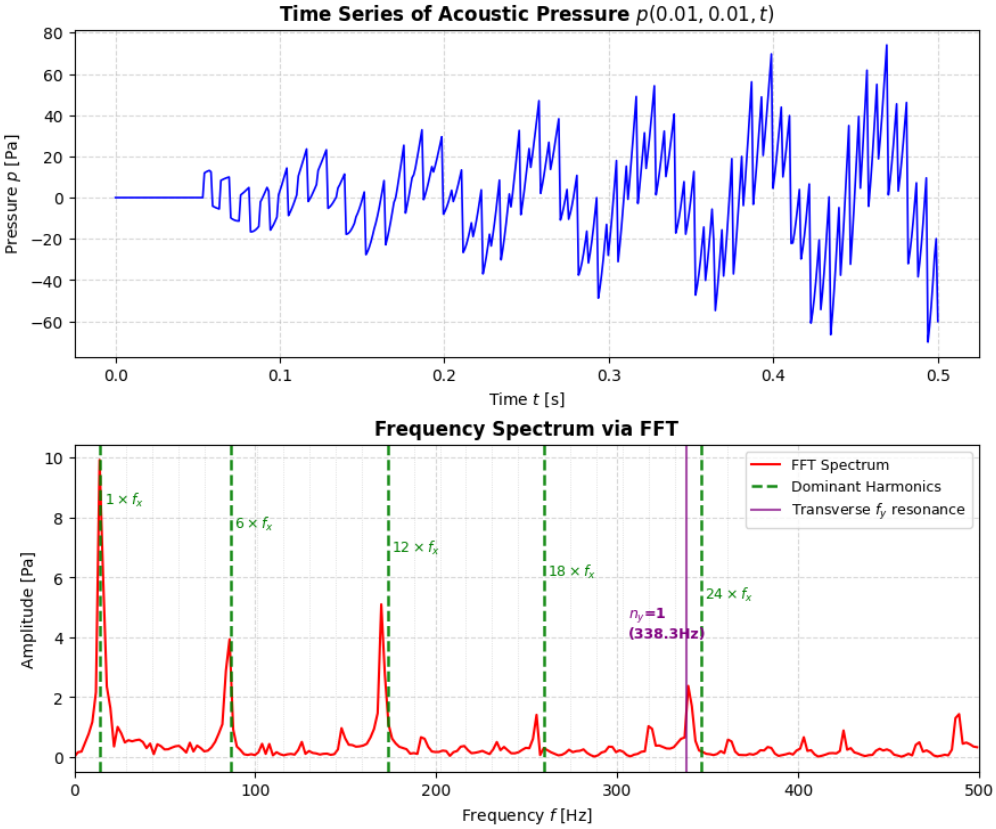

Fig. 2 Numerical Calculation Results

5. Conclusion

Research on automobile whistling and suction sounds has been conducted in the past. For cavity resonance, a type of whistling sound, the cavity resonance frequency has been determined using Rossiter's empirical equation. Therefore, we limited our study to the two-dimensional case and clarified the physical phenomena that arise by solving a set of partial differential equations that explain the phenomenon. As a result, we found that the horizontal resonance frequency becomes proportional to the speed of sound as the mainstream velocity increases, and the vertical resonance frequency decreases as the mainstream velocity increases, but when the Mach number exceeds 1, the resonance frequency no longer exists as a real number, and vertical resonance does not occur. Finally, we discussed the conditions under which resonance increases. Finally, we were able to confirm the conditions under which resonance increases through numerical calculations.

References

Calvo, J. A., Diaz, V., & San Roman, J. L. (2005). *Controlling the turbocharger whistling noise in diesel engines.* International Journal of Vehicle Noise and Vibration, Vol. 2, No. 1. doi:https://doi.org/10.1504/IJVNV.2006.008524

Chien-Hsiung, T., Lung-Ming , F., Chang-Hsien , T., Yen-Loung , H., & Jik-Chang , L. (2009). *Computational aero-acoustic analysis of a passenger car with a rear spoiler.* Applied Mathematical Modelling, Volume 33, Issue 9. doi:https://doi.org/10.1016/j.apm.2008.12.004

George, A. R. (1990). *Automobile Aerodynamic Noise.* SAE Transactions, Vol. 99, Section 6. Retrieved from http://www.jstor.org/stable/44553993

Jagtiani, H. (1972). *The Objective Method of Evaluating Aspiration Wind Noise.* SAE Technical Paper 720506. doi:https://doi.org/10.4271/720506

Jung, W., & Oh, S. (1995). *The Influence of Vehicle Elements to Aspiration Wind Noise.* SAE Technical Paper 950624. doi:https://doi.org/10.4271/950624

Münder, M., & Carbon, C.-C. (2022). *Howl, whirr, and whistle: The perception of electric powertrain noise and its importance for perceived quality in electrified vehicles.* Applied Acoustics, Volume 185. doi:https://doi.org/10.1016/j.apacoust.2021.108412

Oettle, N., & Sims-Williams, D. (2017). *Automotive aeroacoustics: An overview.* Journal of Automobile Engineering, Volume 231, Issue 9. doi:https://doi.org/10.1177/0954407017695147

Qatu, M. S., Abdelhamid, M. K., Pang, J., & Sheng, G. (2009). *Overview of automotive noise and vibration.* International Journal of Vehicle Noise and Vibration, Vol. 5, No. 1-2. doi:https://doi.org/10.1504/IJVNV.2009.029187

Wang, Q., Chen, X., & Zhang, Y. (2021). *An Overview of Automotive Wind Noise and Buffeting Active Control.* SAE International Journal of Vehicle Dynamics, Stability, and NVH, 5(4). doi:https://doi.org/10.4271/10-05-04-0030

Zhang, F., Meng, W., Li, X., & Zheng, C. (2022). *A vehicle whistle database for evaluation of outdoor acoustic source localization and tracking using an intermediate-sized microphone array.* Applied Acoustics, Volume 201. doi:https://doi.org/10.1016/j.apacoust.2022.109113